Influence of Mass Transfer in Distillation: Residue Curves and Total Reflux

R. Taylor
Dept. of Chemical Engineering, Clarkson University, Potsdam, NY 13699

R. Baur and R. Krishna
Dept. of Chemical Engineering, University of Amsterdam, 1018 WV Amsterdam, The Netherlands

DOI 10.1002/aic.10278
Published online in Wiley InterScience (www.interscience.wiley.com).

The relationship is explored between residue curves and composition trajectories in tray and packed distillation columns. The standard model for residue curves as described by, for example, Doherty and Malone is completely consistent, and that published attempts to modify this model to take into account mass transfer effects are flawed. The packed and tray column composition trajectories at total reflux collapse onto the residue curves when each species in the vapor phase has an identical facility for mass transfer (and there is no resistance to mass transfer in the liquid phase). The stationary points of a residue curve map (RCM) and a composition trajectory map (CTM) are the same (pure components and azeotropes). Thus, mass transfer effects do not change the basic structure of the RCM. However, distillation boundaries computed from a mass transfer model are not, in general, identical to those in the RCM. Differences between residue curves and composition trajectories are characterized by the relative length of and angle between the two composition vectors. The relative length of the composition vectors characterizes the separation process and can be best understood as an average efficiency for a multicomponent mixture. For a binary system in a tray column the new efficiency is equal to the Murphree efficiency. For a binary system in a packed column the vector average efficiency is equal to the overall number of transfer units. The average efficiency may also be viewed as the local ratio of the arc length of the actual composition profile to the arc length of the composition trajectory for a reference (virtual) column in which all species have the same facility for mass transfer. The reference composition profile is coincident with a residue curve. © 2004 American Institute of Chemical Engineers *AIChE J,* 50: 3134–3148, 2004

Keywords: residue curve maps, distillation lines, distillation boundaries, mass transfer, Maxwell–Stefan formulation, efficiency, tray columns, packed columns

Introduction

"*The least complicated of all distillation processes is the simple distillation, or open evaporation of a mixture. The liquid is boiled and the vapors are removed from contact with the liquid as soon as they are formed. Thus, the composition of the liquid will change continuously with time, since the vapors are always richer in the more volatile components than the liquid from which they came. The trajectory of the liquid compositions starting from some initial point is called a residue curve; the collection of all such curves for a given mixture is called a residue curve map.*"

This paragraph, taken from *Conceptual Design of Distillation Systems* by Doherty and Malone[1] perfectly describes a tool that has become increasingly important in modern process synthesis and design. Residue curves are closely related to the

Correspondence concerning this article should be addressed to R. Taylor at taylor@clarkson.edu.

© 2004 American Institute of Chemical Engineers

composition profiles in distillation columns.[1] A residue curve map (RCM) can be a valuable aid in the determination of the feasibility of separation sequences.

Although not stated in the above-cited quotation, it is generally understood that the vapors referred to are in equilibrium with the liquid phase. Indeed, it is common practice to assume that the vapor and liquid phases are in equilibrium with each other in the computer-based simulation and design of distillation columns. Real distillation processes, however, nearly always operate away from equilibrium. In fact, the degree of separation actually attained depends on the rates of mass transfer between vapor and liquid phases—rates that depend on the extent to which the two phases are *not* in equilibrium.

For some time it has been possible to simulate distillation and absorption because the mass-transfer rate–based operations they really are using have become known as *nonequilibrium* (NEQ) or *rate-based* models.[2] It is the purpose of this paper to explore the relationships between residue curves and composition trajectories in tray and packed distillation columns when the latter two are computed with a mass transfer rate–based model and identify the circumstances in which residue curves and composition trajectories are essentially identical. We will show that, although mass transfer does not change the basic structure of conventional residue curve maps, mass transfer may alter the precise location of distillation boundaries. We shall find that differences between residue curves and composition trajectories are quantified by a quantity that we call the *geometric average efficiency* [which for binary distillation in tray columns is identical to the Murphree efficiency, and for binary systems in packed columns is closely related to the height equivalent to a theoretical plate (HETP)].

A Unified Framework for Distillation Composition Curves

Residue curves

The starting point for the construction of a residue curve is the differential material balance for species i in the liquid phase

$$\frac{d(Mx_i)}{dt} = -Vy_i \tag{1}$$

where M is the number of moles of liquid and V is the molar flow rate of vapor leaving the system. This equation may be summed over the species index to yield the total material balance. The derivative in Eq. 1 can then be expanded and combined with the total material to give

$$\frac{dx_i}{d\tau} = x_i - y_i \tag{2}$$

where τ is a "warped" time that incorporates the vapor flow rate and molar liquid holdup.[1]

To be able to integrate these equations we need to say something about how the vapor and liquid compositions are related. It is common to assume that the vapor and liquid mole fractions are related through the familiar equation of phase equilibrium

$$y_i = K_i x_i \qquad i = 1, 2, \ldots, n \tag{3}$$

where K represents the so-called K-values or equilibrium ratios. It must suffice to note that the K-values are, in general, complicated functions of the composition of both phases (x_j, $j = 1, \ldots, n$ and y_j, $j = 1, \ldots, n$), temperature (T), and pressure (P). Armed with an appropriate model for the K-values, an additional equation that forces the mole fractions to sum to unity, and an appropriate numerical method, we may integrate these equations from a variety of initial compositions to create a residue curve map.

Mass transfer in multicomponent systems

The rates of mass transfer across a phase interface such as those encountered in real distillation columns (or, indeed, in an open evaporation) actually are determined by the extent to which the phases are *not* in equilibrium with each other. We consider here mass transfer across the interface separating vapor and liquid phases.

It is normal in mass transfer modeling to assume continuity of the molar fluxes across the interface

$$N_i^L = N_i^V \tag{4}$$

The molar fluxes are composed of diffusive and convective fluxes:

$$N_i^L = J_i^L + x_i^L N_t^L = N_i = J_i^V + y_i^V N_t^V = N_i^V \tag{5}$$

where N_t is the total molar flux

$$N_t = \sum_{i=1}^{n} N_i \tag{6}$$

Mass transfer in multicomponent systems is properly modeled by the Maxwell–Stefan (M-S) equations.[3] For the present purposes it suffices to use the following approximations:

$$-\Delta x_i = \sum_{k=1}^{n} \frac{\bar{x}_i N_k^L - \bar{x}_k N_i^L}{c_t^L \kappa_{i,k}^L} \tag{7}$$

$$-\Delta y_i = \sum_{k=1}^{n} \frac{\bar{y}_i N_k^V - \bar{y}_k N_i^V}{c_t^V \kappa_{i,k}^V} \tag{8}$$

where $\kappa_{i,k}^{\alpha}$ is the M-S binary pair mass transfer coefficient in the α phase and c_t^{α} is the molar α-phase density. Δy_i and Δx_i are the mole fraction differences in the vapor and liquid films assumed to exist on each side of the phase interface. We have also ignored thermodynamic corrections attributed to thermodynamic nonideality in writing these equations. The neglect of these terms does not change our results in any significant way.

To complete the picture we may need to consider energy transfer across the vapor liquid interface

$$\sum_{i=1}^{n} N_i \Delta H_{i,vap} + q^V - q^L = 0 \tag{9}$$

where the heat fluxes are given by

$$q^V = h^V(T^I - T^V) \qquad q^L = h^L(T^L - T^I) \tag{10}$$

and where $\Delta H_{i,vap}$ is the molar latent heat of vaporization. If the latent heats are equal (as often is assumed to be true in distillation), *and* we ignore the sensible heat terms (because they are quite small compared to the convective energy flux), then the energy balance simplifies to

$$\Delta H_{vap} \sum_{i=1}^{c} N_i = \Delta H_{vap} N_t = 0 \tag{11}$$

from which it follows that the total molar flux must be zero under these conditions.

It is sometimes desirable to cast the M-S equations in matrix form as (see Section 11.5 of Taylor and Krishna[3])

$$(J^V) = c_t^V[k^V](\Delta y) \qquad (J^L) = c_t^L[k^L](\Delta x) \tag{12}$$

where $[k^\alpha]$ are square matrices of dimension $n - 1$ of multicomponent mass transfer coefficients for the phases identified by the superscript ($\alpha \in \{V, L\}$). These matrices are defined by

$$[k^\alpha] = [R^\alpha]^{-1} \tag{13}$$

The elements of the $[R]$ matrices are defined in terms of the binary M-S mass transfer coefficients by

$$R_{i,i}^\alpha = \frac{z_i^\alpha}{\kappa_{i,c}^\alpha} + \sum_{\substack{k=1 \\ k \neq i}}^{c} \frac{z_k^\alpha}{\kappa_{i,k}^\alpha} \qquad R_{i,j}^\alpha = -z_i^\alpha \left(\frac{1}{\kappa_{i,j}^\alpha} - \frac{1}{\kappa_{i,c}^\alpha} \right) \tag{14}$$

where z_i^α is the mole fraction of species i in the α phase ($z \in \{x, y\}$).

Equations 12 sometimes are combined to give (see Section 7.3.1 of Taylor and Krishna[3])

$$(J^V) = c_t^V[K_{OV}](y^V - y^*) \tag{15}$$

where (y^*) is a column matrix of vapor mole fractions that would be in equilibrium with the bulk liquid and $(y^* - y^V)$ is the overall driving force for mass transfer. $[K_{OV}]$ is a square matrix of overall mass transfer coefficients that may be calculated from

$$[K_{OV}] = [R^{OV}]^{-1} \tag{16}$$

$$[R^{OV}] = [R^V] + \frac{c_t^V}{c_t^L}[K][R^L] \tag{17}$$

where $[K]$ is a diagonal matrix of equilibrium ratios (K-values).

Equations 15–17 rely on two key assumptions:

(1) The heats of vaporization are the same for all components

(2) The sensible heat terms in the energy balance are negligible in comparison to the latent heat terms.

The first of these restrictions can be dealt with fairly easily using a more complicated version of the addition of resistances formula (Eq. 17) (see Section 7.3.1 of Taylor and Krishna[3]—but which still requires neglect of the sensible heat terms in the energy balance).

It might be supposed that we should take mass transfer into account in the calculation of the residue curves themselves. Toward this end there have been a few recent attempts to develop a framework for the construction of RCMs that explicitly include mass transfer rate equations in the model,[4-6] Such attempts are, as shown in the Appendix, seriously flawed; mass transfer rate equations have no place in a model for the residue curve map as it is described by Doherty and Malone.[1]

Packed columns

For continuous contact equipment the component material balances for the vapor phase can be expressed in matrix form as (see Section 12.3.1 of Taylor and Krishna[3])

$$\frac{d(y^V)}{d\eta} = [\mathbb{N}_{OV}](y^* - y^V) \tag{18}$$

where η is a dimensionless height coordinate and (y^*) is the column matrix of mole fractions of a vapor in equilibrium with the bulk liquid. $[\mathbb{N}_{OV}]$ is a matrix of numbers of transfer units for a packed column defined by

$$[\mathbb{N}_{OV}] = c_t^V[K_{OV}]a' A_c h/V \tag{19}$$

where a' is the interfacial area per unit volume, A_c is the cross-sectional area of the column, and h is the height of the packed section. At total reflux the changes in composition of the two phases are given by

$$dx_i^L = -dy_i^V \qquad x_i^L = y_i^V \tag{20}$$

Thus, we may rewrite Eq. 18 in a form similar to Eq. 2 for the residue curves

$$\frac{d(x^L)}{d\eta} = [\mathbb{N}_{OV}](x^L - y^*) \tag{21}$$

Tray columns

The composition of the vapor streams entering and leaving a distillation tray are given by (see Section 13.3.1 of Taylor and Krishna[3] for the derivation)

$$(y_L - y_E) = \{[I] - [Q]\}(y^* - y_E) \tag{22}$$

where the subscripts E and L refer to the entering and leaving streams and $[Q]$ is a square matrix defined by

$$[Q] = \exp(-[\mathbb{N}_{OV}]) \tag{23}$$

where $[\mathbb{N}_{OV}]$ is a matrix of numbers of transfer units here defined by

$$[\mathbb{N}_{OV}] = c_t^V [K_{OV}] a' A_c h_f / V \tag{24}$$

where a' is the interfacial area per unit volume of froth, A_b is the bubbling area of the tray, and h_f is the froth height.

Equation 22 relies on the assumption that $[\mathbb{N}_{OV}]$ can be assumed constant over the froth height, an assumption commonly made in modeling mass transfer in distillation. We further assume that the liquid phase is well mixed in the (horizontal) flow direction, but note that it is possible to relax this assumption and obtain an expression with the form of Eq. 22 with Eq. 23 replaced by a more complicated result (see Eqs. 13.3.20 and following of Taylor and Krishna[3]).

The term on the lefthand side of Eq. 22 is the actual change in composition over the froth height. We may exprress this term as

$$(y_L - y_E) = \frac{\Delta(y^V)}{\Delta\eta} \tag{25}$$

where $\Delta\eta$ is a change in stage number ($\Delta\eta = 1$ here). To obtain a set of autonomous differential equations we approximate the composition difference with differentials

$$\frac{\Delta(y^V)}{\Delta\eta} \approx \frac{d(y^V)}{d\eta} \tag{26}$$

Now, at total reflux in a tray column

$$(x^L) = (y_E) \qquad d(x^L) = -d(y^V) \tag{27}$$

Thus, Eq. 22 could be approximated by

$$\frac{d(x^L)}{d\eta} = \{[I] - [Q]\}(x^L - y^*) \tag{28}$$

A unified model

We now see that the equations that describe residue curves and, under certain conditions, the composition trajectories in both tray and packed distillation columns can be written in compact $n - 1$ dimensional matrix form as

$$\frac{d(x)}{d\eta} = [\Omega](x - y^*) \tag{29}$$

where η is a dimensionless time or distance coordinate. In addition, $[\Omega]$ is a square matrix of order $n - 1$ defined as follows.

For Residue Curves

$$[\Omega] = [I] \tag{30}$$

For Tray Columns

$$[\Omega] = [I] - [Q] \qquad [Q] = \exp(-[\mathbb{N}_{OV}]) \tag{31}$$

For Packed Columns

$$[\Omega] = [\mathbb{N}_{OV}] \tag{32}$$

For both tray and packed columns $[\mathbb{N}_{OV}]$ may be calculated from the addition of resistances formula (cf. Eq. 17 and Eqs. 13.3.20 and following of Taylor and Krishna[3])

$$[\mathbb{N}_{OV}]^{-1} = [\mathbb{N}_V]^{-1} + \frac{V}{L}[K][\mathbb{N}_L]^{-1} \tag{33}$$

The matrices for the number of transfer units for the vapor and liquid phases ($[\mathbb{N}_V]$ and $[\mathbb{N}_L]$, respectively) are defined for tray columns by (cf. Eqs. 14)

$$\mathbb{N}^{-1}_{\alpha:i,i} = \frac{z_i^\alpha}{\mathcal{N}^\alpha_{i,c}} + \sum_{\substack{k=1 \\ k\neq i}}^{c} \frac{z_k^\alpha}{\mathcal{N}^\alpha_{i,k}} \qquad \mathbb{N}^{-1}_{\alpha:i,j} = -z_i^\alpha \left(\frac{1}{\mathcal{N}^\alpha_{i,j}} - \frac{1}{\mathcal{N}^\alpha_{i,c}} \right) \tag{34}$$

The superscript -1 indicates that these expressions are for the elements of the inverse matrices $[\mathbb{N}_\alpha]^{-1}$. $\mathcal{N}^\alpha_{i,j}$ represents the numbers of transfer units for the binary pair of components identified by the subscript letters in the phase identified by the superscript.

For packed columns the formulation here is essentially equivalent to that presented by Pelkonen et al.[7]

The formulae for tray and packed distillation columns rest on a number of assumptions:

(1) Total reflux operation.

(2) The molar flows in the column are constant (this requires the latent heats to be equal and the sensible heat fluxes to be negligible in comparison to the enthalpy fluxes).

(3) The temperature is assumed to be the boiling point of the liquid mixture (because, otherwise, it would be undefined by the equations given above).

(4) The vapor phase rises through the column in plug flow.

(5) The liquid phase is well mixed laterally.

Most of these assumptions can be relaxed fairly easily. Consideration of the effects of nonconstant molar flows (assumption 2 above) simply leads to a more complicated formula for the matrix of overall mass transfer coefficients (see Section 7.3.1 of Taylor and Krishna[3]). We may also consider more realistic liquid flow models (these lead to more complicated relationships for $[\Omega]$; see, for example, Section 13.3.3 of Taylor and Krishna[3]). Sensible heat transfer between phases is very small relative to latent heat transfers and the restriction implied by assumption 3 above is not at all serious. The most serious limitation here is that of total reflux operation; in fact, it is straightforward (but beyond the scope of this paper) to consider finite reflux operation. In a companion paper we look in detail at the (sometimes significant) impact of mass transfer on distillation process feasibility and column design.

Some analysis

The $\mathcal{N}_{i,j}^{\alpha}$ are positive (all *i–j* combinations). It can be shown that the matrices of transfer units are positive semidefinite.[3] $[Q]$ is also positive semidefinite. Thus, the stationary points of a composition trajectory map (CTM) for tray or packed columns are the same as the stationary points of the residue curve map (RCM) (the pure components and azeotropes). In other words, a CTM that accounts for mass transfer effects has the basic structure of the RCM. For the CTM to be identical to the RCM requires the $[\Omega]$ matrix to be diagonal with all elements on the main diagonal equal ($[\Omega]$ must be a scalar times the identity matrix). Let us see whether this is possible.

In the event that the binary numbers of transfer units all have the same value ($\mathcal{N}_{i,k}^{\alpha} = \mathcal{N}^{\alpha}$, $i \neq k = 1, 2, \ldots, n$; $\alpha \in \{V, L\}$) the resistance matrices are diagonal

$$[\mathbb{N}^V] = \mathcal{N}^V[I] \qquad [\mathbb{N}^L] = \mathcal{N}^L[I] \tag{35}$$

where $[I]$ is the identity matrix. $[\mathbb{N}_{OV}]$ will also be diagonal with elements given by

$$\frac{1}{\mathcal{N}_{i,OV}} = \frac{1}{\mathcal{N}^V} + \frac{K_i V/L}{\mathcal{N}^L} \tag{36}$$

The equilibrium ratios will have different values (except at azeotropes when all of them are unity—a singularly uninteresting state of affairs, given that there is no mass transfer under those conditions anyway). Thus, the assumption of equal mass transfer coefficients in both phases is not sufficient for $[\Omega]$ to take the required form.

However, if we also neglect the resistance to mass transfer in the liquid phase, then $\mathcal{N}^L \to \infty$ and $[\mathbb{N}^L]^{-1} \to [0]$. Under these conditions the matrix of transfer units does indeed become a scalar multiplied by the identity matrix and we can write

$$[\mathbb{N}_{OV}] = [\mathbb{N}_V] = \mathcal{N}_{OV}[I] \tag{37}$$

where $\mathcal{N}_{OV} = \kappa a' H/u^V$ is the representative number of transfer units for the system. If, further, we define a new coordinate variable as $\eta^* = \mathcal{N}_{OV}\eta$, then Eq. 21 becomes (assuming, again as is commonly done, that $\mathcal{N}_{OV}$ is constant)

$$\frac{d(x^L)}{d\eta^*} = (x^L - y^*) \tag{38}$$

This is the matrix form of Eq. 2 for the residue curves! Thus, to recover the residue curve the *differences* between the binary numbers of transfer units (or mass transfer coefficients) have to vanish. This special case is formally equivalent to the conventional HTU/NTU (height of transfer unit/number of transfer units) approach (see Section 7.5 of Seader and Henley[8]). Pelkonen et al.[7] derived similar equations as part of their investigation into mass transfer in packed columns and drew the same conclusion.

For a tray column, the same set of assumptions ($\mathcal{N}_{i,k}^{V} = \mathcal{N}^{V}$, $i \neq k = 1, 2, \ldots, n$, neglecting the liquid phase resistance) in Eqs. 29 and 31 yields

$$[\Omega] = (1 - e^{-\mathcal{N}_{OV}})[I] \tag{39}$$

The scalar multiplier $(1 - e^{-\mathcal{N}_{OV}})$ is the Murphree efficiency, which is the same for all components in this case. For this case we may define a new coordinate variable as $\tau = [1 - \exp(-\mathcal{N}_{OV})]\eta$, in which case Eq. 29 collapses to Eq. 38.

Equations 29 and 31 for tray columns also become equivalent to the residue curves when $[Q] \to [0]$ (a null matrix). From Eq. 23 we see that this requires $[\mathbb{N}_{OV}] \to [\infty]$. This, in turn, requires that $\mathcal{N}_{i,k}^{V} \to \infty$ ($i, k = 1, 2, \ldots, n$), in which case the efficiencies of all components are unity and each tray represents an equilibrium stage. For the more usual case of finite but unequal mass transfer coefficients $[\Omega]$ for a tray column is analogous to a square matrix of efficiency-like quantities, $(n - 1)^2$ in number. These entities are not the conventional Murphree efficiencies (although there is a simple relationship between them; see Chapter 13 of Taylor and Krishna[3]).

Computational procedure

To compute the composition trajectories and residue curves we need to augment the differential Eqs. 29 with Eq. 31 or Eq. 32 and Eqs. 33 and 34 for the matrix of transfer units, and an appropriate correlation for the binary numbers of transfer units. Equation 3, with an appropriate thermodynamic model, is needed to compute the equilibrium vapor composition (y^*) and bubble point temperature. This leads to a set of differential–algebraic equations (DAEs). In the calculations carried out for this investigation we integrated the set of DAEs using BESIRK,[9] which is a semi-implicit Runge–Kutta method originally developed by Michelsen[10] and extended with an extrapolation scheme,[11] thereby improving the efficiency of solving the DAE problem. A Taylor approximation has been used for the evaluation of exponential matrix in Eq. 23.

It must be noted that the matrix of overall mass transfer coefficients (or that of overall numbers of transfer units) needs to be reevaluated at every step of the calculation. The structure of these matrices is a function of composition and changes as the boundaries of composition space are approached. If the matrix of overall mass transfer coefficients is maintained constant, having been evaluated just once at some representative average composition, then it is possible for the composition trajectories to leave meaningful composition space ($0 \leq x_i \leq 1$, $i = 1, 2, \ldots, n$).

Illustrative Examples

It follows from the above discussion that to investigate the effects of finite mass transfer rates on composition trajectories in distillation columns (at total reflux) we need to consider the influence of *differences* between the component efficiencies, as manifested by differences between binary M-S mass transfer coefficients. Differences between binary mass transfer coefficients occur solely because of differences between the binary M-S diffusion coefficients. The resistance to mass transfer in the liquid phase is ignored in what follows, and the numbers of binary transfer units for the vapor phase estimated from a simple model

$$\mathcal{N}_{i,j} = C_1\left(\frac{D_{i,j}}{D_{ref}}\right)^{C_2} \tag{40}$$

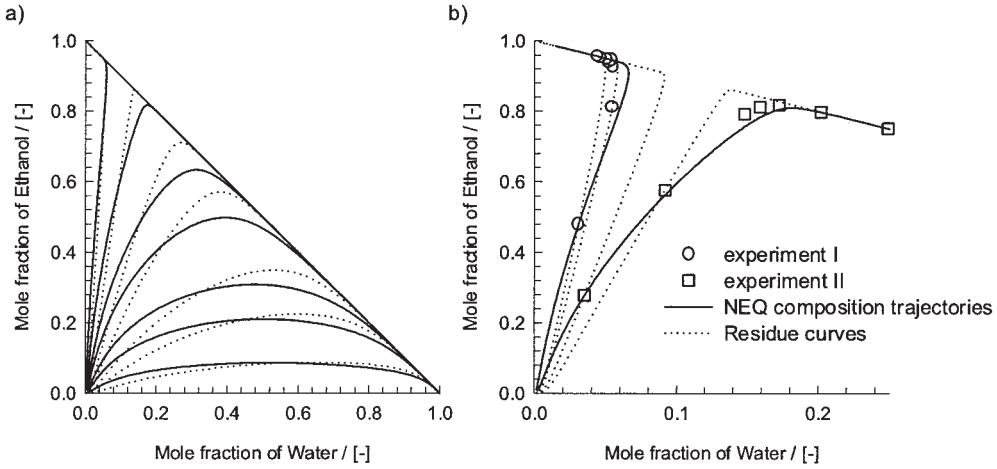

Figure 1. Equilibrium residue curves (broken lines) and nonequilibrium composition trajectories (solid lines) for the ethanol–water–acetone system.

Data from Springer et al.[12]

where D_{ref} is a reference diffusion coefficient; a value of 1×10^{-5} m^2/s was used here. The influence of various mixture physical properties, column design, and operational variables are lumped into C_1 to which we will later assign a numerical value. The constant C_2 is a parameter of the system and the hydrodynamic regime in the column. A value of 0.5 is suggested (by mass transfer theory as well as by empirical data) for distillation in the spray/froth regime on trays. A value of unity is needed for the bubbling regime.[12] The parameter C_1 depends on the operating conditions and can be manipulated by changing such parameters as the residence time and bubble size. In a real distillation column this parameter may not be constant over the entire height of the device.

Ethanol–water–acetone in a tray column

Our first illustration is with the ethanol–water–acetone system. The ratio of largest to smallest vapor phase diffusion coefficient is about 3 in this system. This is typical of systems encountered in distillation operations (as opposed to gas absorption where the ratio of largest to smallest coefficient can be somewhat higher).

Figure 1 shows the residue curves and composition vectors for the ethanol–water–acetone system determined using the procedure described above with the mass transfer coefficients estimated from Eq. 40 with $C_1 = 0.65$ and $C_2 = 1$. Figure 1b shows measured composition trajectories from Springer et al.[12] and computed composition trajectories on either side of the distillation boundary connecting the pure acetone vertex to the ethanol–water binary azeotrope. Data from some additional experiments on either side of the distillation boundary are shown in Figure 2. Also shown is the computed equilibrium distillation boundary. The important points here are as follows:

- The nonequilibrium and equilibrium distillation boundaries are not always the same (although their end points are identical).
- The nonequilibrium model is a much more accurate representation of the actual composition trajectory than is the equivalent residue curve.

The component Murphree efficiencies are easily computed from the results of a composition trajectory calculation. For a three-component system we have

$$E_1^{MV} = \frac{\Delta y_{1,L}}{\Delta y_1^*} \qquad E_2^{MV} = \frac{\Delta y_{2,L}}{\Delta y_2^*}$$

$$E_3^{MV} = \frac{\Delta y_{3,L}}{\Delta y_3^*} = \frac{\Delta y_1^* E_1^{MV} + \Delta y_2^* E_2^{MV}}{\Delta y_1^* + \Delta y_2^*} \quad (41)$$

where $\Delta y_{i,L} = y_{i,L} - y_{i,E} = y_{i,L} - x_i$ and $\Delta y_i^* = y_i^* - y_{i,E} = y_i^* - x_i$. In general, these component efficiencies are not the same for each component; they are also not required to take values between zero and one because they are for a binary system and

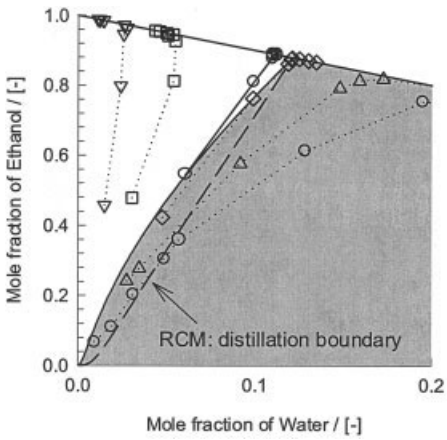

Figure 2. Experimental composition trajectories and nonequilibrium and equilibrium distillation boundaries for the ethanol–water–acetone system.

The white and gray regions lie on opposite sides of the nonequilibrium distillation boundary. Data from Springer et al.[12]

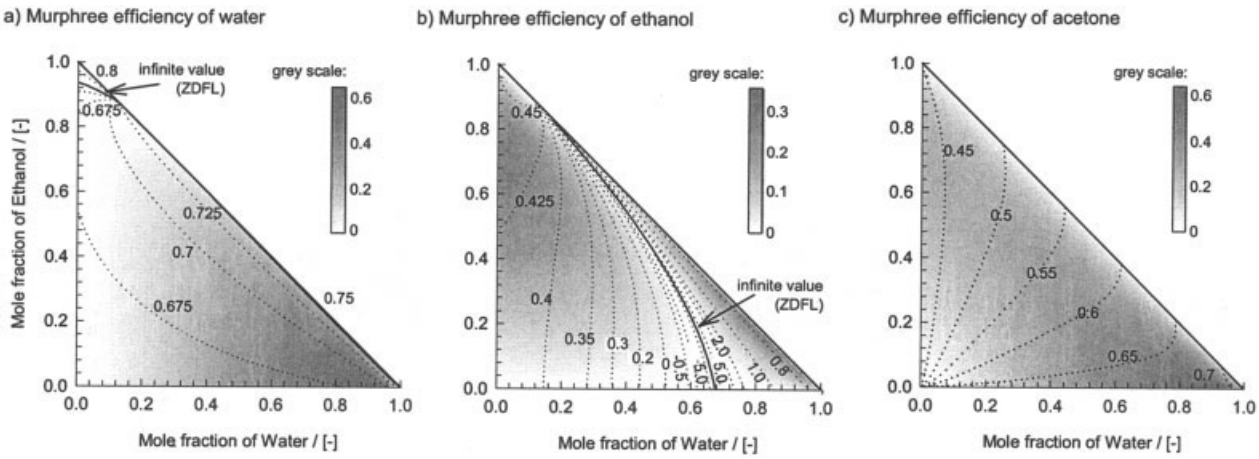

Figure 3. Component Murphree efficiencies of the ethanol–water–acetone system.

Shading denotes the magnitude of the overall driving force $x - y^*$. The zero driving force line corresponds to an inflection in the composition trajectories.

may indeed be found anywhere in the range $-\infty < E_i^{MV} < \infty$ (there is abundant experimental evidence that demonstrates the truth of this statement; see the compilation in Chapter 13 of Taylor and Krishna[3]).

Figure 3 shows the calculated component efficiencies and overall driving forces for this system. In the diagrams for water and ethanol we see a line where the overall driving force is zero (the ZDFL: zero driving force line); a short line near the top corner for water and a long downward right sloping line for ethanol. There is no ZDFL for acetone (except along the ethanol–water boundary line). The component efficiencies pass through a discontinuity along that line. On one side of the ZDFL the efficiencies are greater than unity and on the other side they are less than zero. In a large part of the composition triangle the efficiency of water is about 70%, but the efficiency of ethanol is much lower almost everywhere except for the corner where water is in high concentrations. The efficiency of acetone varies between 45 and 70%. The fact that the component efficiencies change sign on either side of the ZDFL means there should be a change in direction of the composition curves as they cut the ZDFL.

The unbounded nature of the component efficiencies suggests that these quantities are perhaps not the best indicators of the differences between equilibrium (residue) curves and composition trajectories. The arithmetic average Murphree efficiency also is excessively sensitive to very large positive or negative efficiencies that can arise when one of the component driving forces is vanishingly small; something better is needed.

A new type of distillation efficiency

The fragment of composition space in Figure 4 clearly shows that the differences between residue curves and composition trajectories are characterized by the angle between the composition vectors and by their relative length. The latter, here denoted by the Greek letter ε, is given by

$$\varepsilon = \frac{\sqrt{\sum_{i=1}^{n} (\Delta y_{i,L})^2}}{\sqrt{\sum_{i=1}^{n} (\Delta y_i^*)^2}} \tag{42}$$

For a binary system Eq. 42 simplifies as follows

$$\varepsilon = \frac{\sqrt{(\Delta y_{1,L})^2 + (\Delta y_{2,L})^2}}{\sqrt{(\Delta y_1^*)^2 + (\Delta y_2^*)^2}} = \frac{\Delta y_{1,L}}{\Delta y_1^*} = E_1^{MV} = E_2^{MV} \tag{43}$$

That is, ε for a binary system is equal to the Murphree efficiencies of the two species. For multicomponent systems, ε can be thought of as an average efficiency for a multicomponent system. Unlike individual component efficiencies in multicomponent systems, ε cannot be negative.

For a ternary system the angle α between the composition change vectors can be calculated from

$$\cos(\alpha) = \frac{\sum_{i=1}^{n} \Delta y_i^* \Delta y_{i,L}}{\sqrt{\sum_{i=1}^{n} (\Delta y_i^*)^2 \sum_{i=1}^{n} (\Delta y_{i,L})^2}} \tag{44}$$

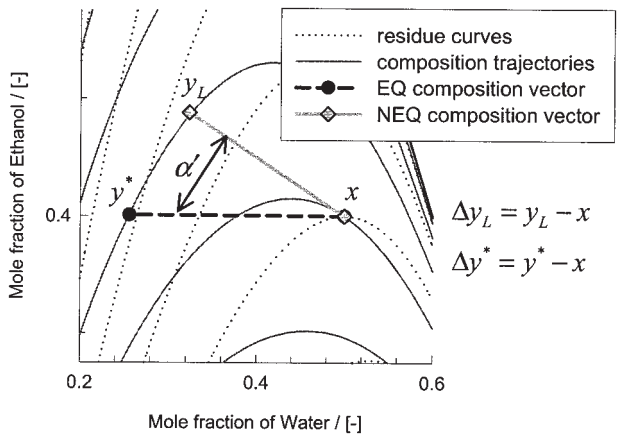

Figure 4. Illustration of the differences between the equilibrium (residue curve) and nonequilibrium composition vectors.

α' is the projection of the angle between these vectors onto the coordinate system used here.

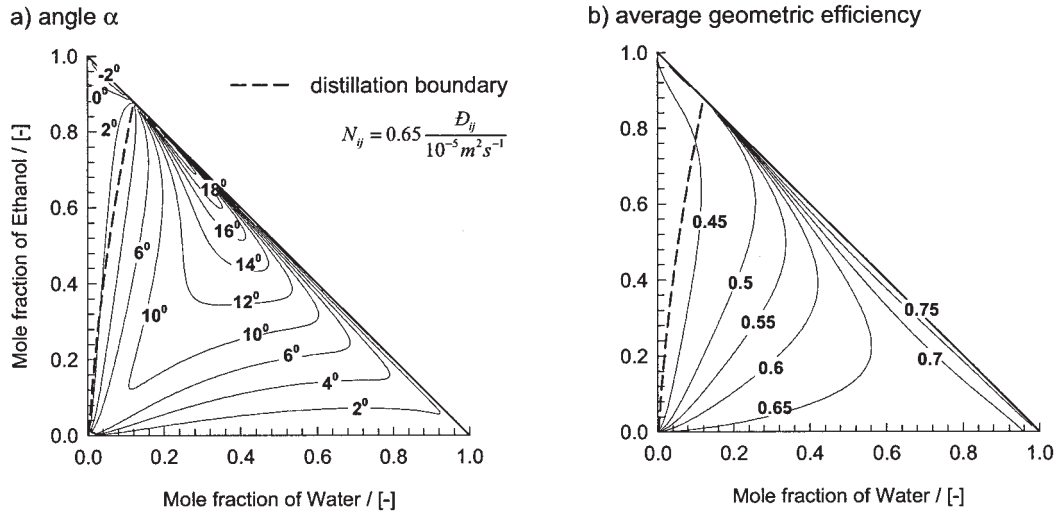

Figure 5. Contour plots for the ethanol–water–acetone system showing the vector angle α and the average efficiency.

Numbers of transfer units calculated from Eq. 40 with $C_1 = 0.65$, $C_2 = 1$.

Contour plots of the composition vector angle and ε for this system are shown in Figure 5. The diagram clearly shows that the angle between the composition vectors is very small at the boundaries of the composition triangle as well as in the vicinity of the distillation boundary (as should be the case, of course). However, there is a much greater influence of mass transfer (as measured by the angle between the vectors) in the central portion of the diagram. In this (and all other illustrations shown here) of the angle between composition vectors we define the angle as positive when $\Delta y_1^* \Delta y_2^* (E_2^{MV} - E_1^{MV}) > 0$.

Figure 6 shows the contour plots for α and ε in which we have again used Eq. 40 for the calculation of the number of transfer units, but in this case $C_2 = 0.5$. This has the effect of making the mass transfer coefficients (numbers of transfer units) more nearly equal. The off-diagonal elements of the matrix of transfer units will be reduced in magnitude compared to the diagonal elements, and the mixture behaves more like one in which all species have an equal facility for mass transfer. In this case α is smaller and ε does not vary so widely over the composition space.

Methanol–water–methylacetate in a tray column

Figure 7 compares the composition trajectories and residue curves for the methanol–water–methylacetate system. This system features two binary azeotropes, methanol–methylacetate and water–methylacetate, that are joined by a distillation boundary.

The portion of composition space near the pure methylacetate vertex that includes the binary azeotropes and distillation boundary is shown in Figure 8. We can see that the distillation boundaries computed from the equilibrium and nonequilibrium

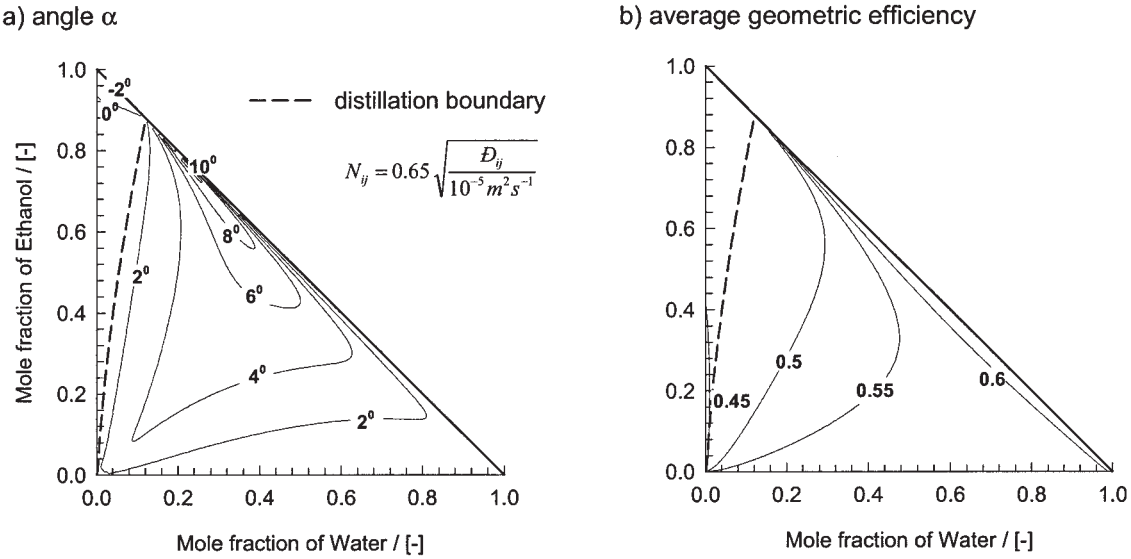

Figure 6. Contour plots for the ethanol–water–acetone system showing the vector angle α and the average efficiency.

Numbers of transfer units calculated from Eq. 40 with $C_1 = 0.65$, $C_2 = 0.5$.

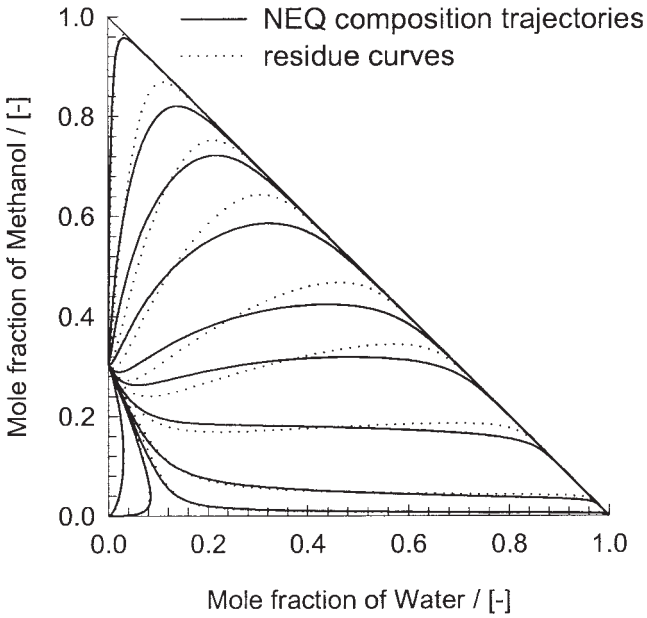

Figure 7. Equilibrium and nonequilibrium composition trajectories for the methanol–water–methylacetate system.

models are different, although their end points are identical (the binary azeotropes). The nonequilibrium profiles in this figure were computed using Eq. 40 for the transfer units with $C_1 = 0.9$ and $C_2 = 1$.

Contour plots for α (left) and ε are shown in Figure 9 for three cases in which $C_1 = 0.9$, $C_1 = 1.5$, and $C_1 = 3$, respectively; $C_2 = 1$ in all three cases. We see here that ε increases as the number of transfer units increases (as it should). ε is close to unity throughout the composition triangle for the case in which $C_1 = 3$, even near the distillation boundary. At the same time, α decreases as the number of transfer units increases. Again, this is at it should be, based on the fact that as the number of transfer units increases the nonequilibrium composition trajectories become more aligned with the equilibrium-based residue curves.

The experimental work of Springer et al.[13] for the water–ethanol–methylacetate system confirms the need for including rigorous Maxwell–Stefan equations in describing the composition trajectories during distillation in a tray distillation column. These experiments also demonstrate that classic EQ distillation boundaries can be crossed.

Efficiencies in a packed column

For a packed column the efficiency, defined by Eq. 42, has a simple and appealing physical significance. The differential arc length of the composition trajectory in composition space is given by

$$ds = \sqrt{\sum_{i=1}^{n} \left[\frac{\partial y_i(\eta)}{\partial \eta}\right]^2}\, d\eta \tag{45}$$

where s is the arc length. For short arc lengths the partial derivatives in Eq. 45 may be assumed to be constant and we may approximate the arc length of the composition trajectory by

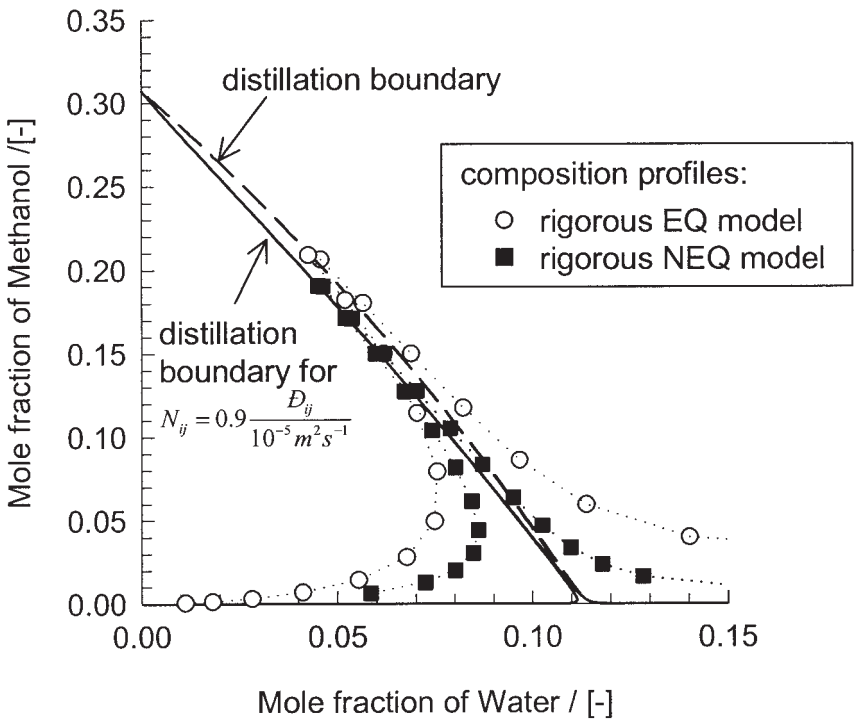

Figure 8. Equilibrium and nonequilibrium distillation boundaries for the methanol–water–methylacetate system.

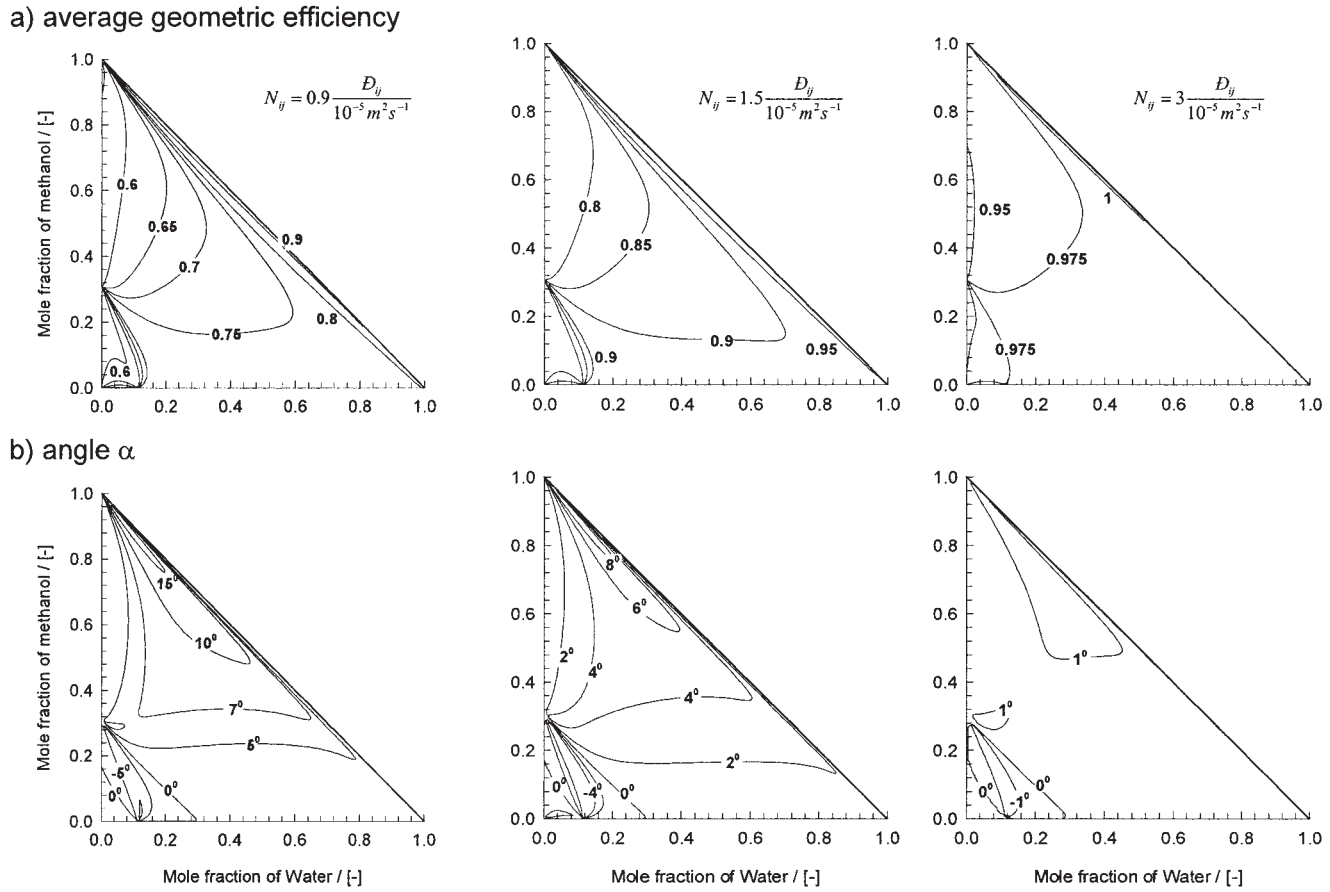

Figure 9. Contour plots for the methanol–water–methylacetate system in a tray column showing the vector angle α (top row) and the geometric average efficiency (bottom row).

Numbers of transfer units calculated from Eq. 40 with three different values of C_1 as shown.

$$\delta s = \sqrt{\sum_{i=1}^{n} (\Delta y_{i,L})^2 \delta\eta} \tag{46}$$

This approximation (and that below) follows from the differential equations that describe the composition curves. The relationship between the arc length and the numerator of Eq. 42 is clear. The denominator is related to the arc length of the composition trajectory for what we refer to as a virtual column, one in which all species have the same facility for mass transfer ($[\Omega] = [\mathbb{N}_{OV}] = \mathcal{N}^+[I]$) and where $\mathcal{N}^+ = \kappa^+ a' H/u^V = 1$. κ^+ is the mass transfer coefficient that makes the number of transfer units for this virtual column equal to unity. The arc length of the composition curve for this virtual column may be approximated by

$$\delta s^+ = \sqrt{\sum_{i=1}^{n} (\Delta y_i^*)^2 \delta\eta^+} \tag{47}$$

Thus, ε simply is the local ratio of the arc length of the composition trajectory to the arc length of the corresponding virtual column: $\varepsilon = \delta s/\delta s^+$ (after making the assumption that the arc length is evaluated over the same height of packing, so $\delta\eta = \delta\eta^+$).

For binary systems in packed columns the efficiency becomes

$$\varepsilon = \frac{\sqrt{2(\mathbb{N}_{OV}\Delta y_1^*)^2}}{\sqrt{2(\mathcal{N}^+\Delta y_1^*)^2}} = \mathbb{N}_{OV} \tag{48}$$

Thus, the HTU is related to the average efficiency by $H_{OV} = H/\mathbb{N}_{OV} = H/\varepsilon$ and assuming that the equilibrium line is straight (with local slope m), we obtain the well-known relations between the NTU, HTU, HETP, and the number of equilibrium stages

$$\text{HETP} = H_{OV} \frac{\ln(m)}{(m-1)} = \frac{H}{\varepsilon} \frac{\ln(m)}{(m-1)} \tag{49}$$

with the number of equivalent theoretical stages given by

$$N^* = \frac{H}{\text{HETP}} = \varepsilon \frac{(m-1)}{\ln(m)} \tag{50}$$

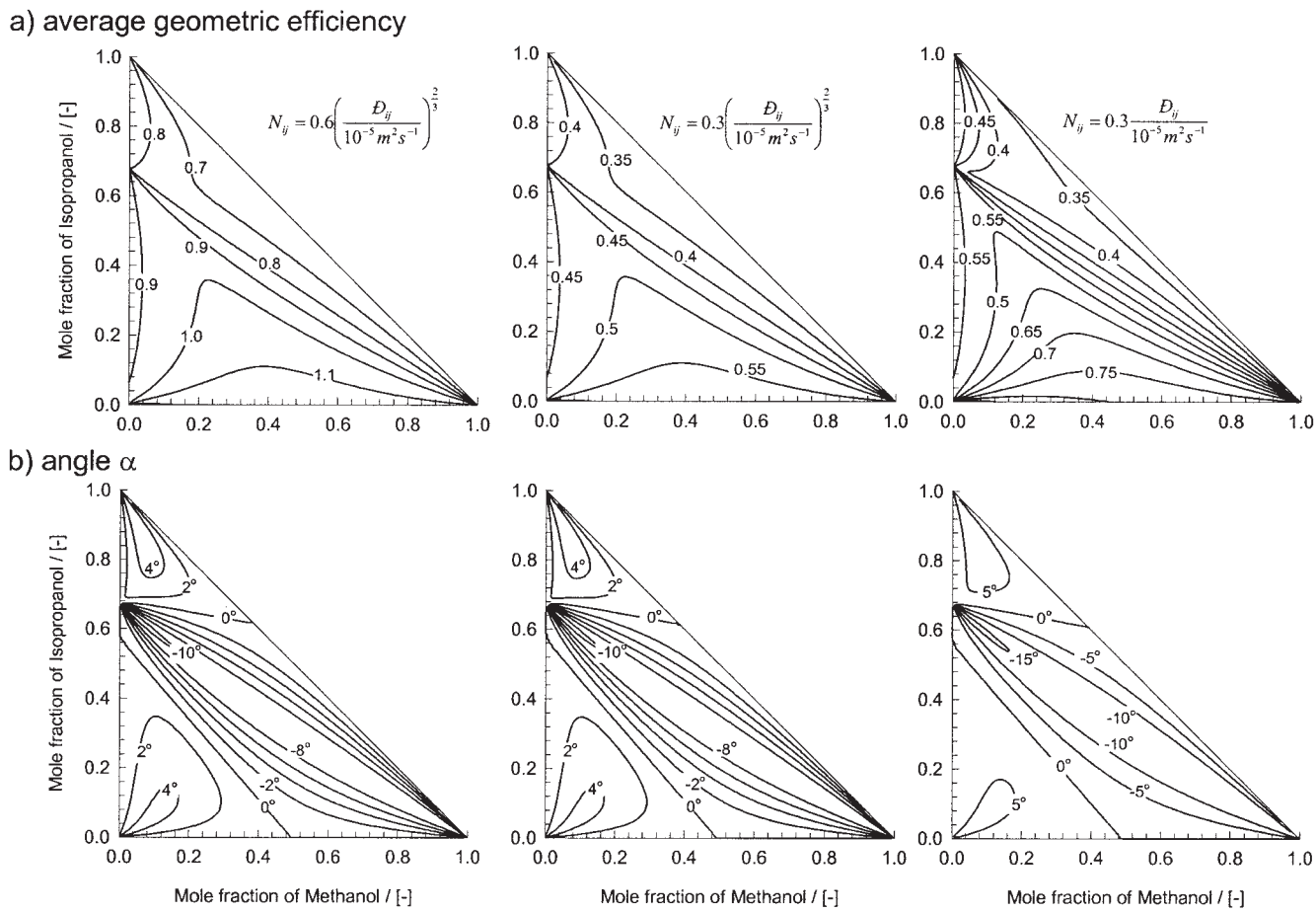

Figure 10. Contour plots for the methanol–water–isopropanol system in a packed column showing the vector angle α (bottom row) and the geometric average efficiency (top row).

Numbers of transfer units calculated from Eq. 40 with three different values of C_1 as shown.

It should be noted that the composition trajectory of the virtual column is coincident with a residue curve. Thus, in a sense, the denominator in the definition of ε is related to the arc length of the corresponding residue curve. It should also be noted that for a tray column the average efficiency can be considered to be the ratio of the arc length of the actual composition curve to the arc length of the composition trajectory in a virtual tray column in which $[\Omega] = E^{+}_{MV}[I]$, where $E^{+}_{MV} = 1 - e^{-\mathcal{N}_{OV}} = 1$. Thus the virtual tray column is an equilibrium stage device and the composition curve for this virtual tray column is also coincident with a residue curve.

Figure 10 shows the average efficiency and the vector angle maps for the methanol–isopropanol–water ternary system in a packed column. As in our illustrations for tray columns we have used a simple correlation, Eq. 40, for the numbers of binary transfer units. The efficiency maps demonstrate that the packed column efficiency is directly proportional to the value of the constant C_1 (this would be expected in view of Eq. 48). The vector angle maps show that the angle between composition vectors depends only on the exponent C_2. In other words, the composition trajectory itself is independent of the parameter C_1. Composition trajectories for the methanol–isopropanol–water ternary system are shown in Figure 11a. This figure provides another illustration of the fact that the distillation boundaries computed from the equilibrium and nonequilibrium models may differ. Composition curves for the methanol–isopropanol–acetone–water quaternary system in a packed column are shown in Figure 11b. Here we see that the nonequilibrium trajectory ends up at the water vertex, whereas the residue curve (corresponding to the composition trajectory for the virtual column) ends at the isopropanol vertex! The experimental data of Pelkonen et al.[7] included in Figure 11 show that the mass transfer model more accurately represents the composition trajectories. The data demonstrate crossing of the EQ distillation boundary and not the NEQ distillation boundary. This emphasizes the need for NEQ modeling to describe the composition trajectories near the boundary region.

Conclusions

The standard model for residue curves as described by, for example, Doherty and Malone,[1] is completely consistent. Published attempts to modify this model to take into account mass transfer effects are flawed. A framework for constructing composition trajectories in tray and packed distillation columns at total reflux and that take into account mass transfer has been described in this paper. For packed columns the procedure is essentially equivalent to that of Pelkonen et al.[7]

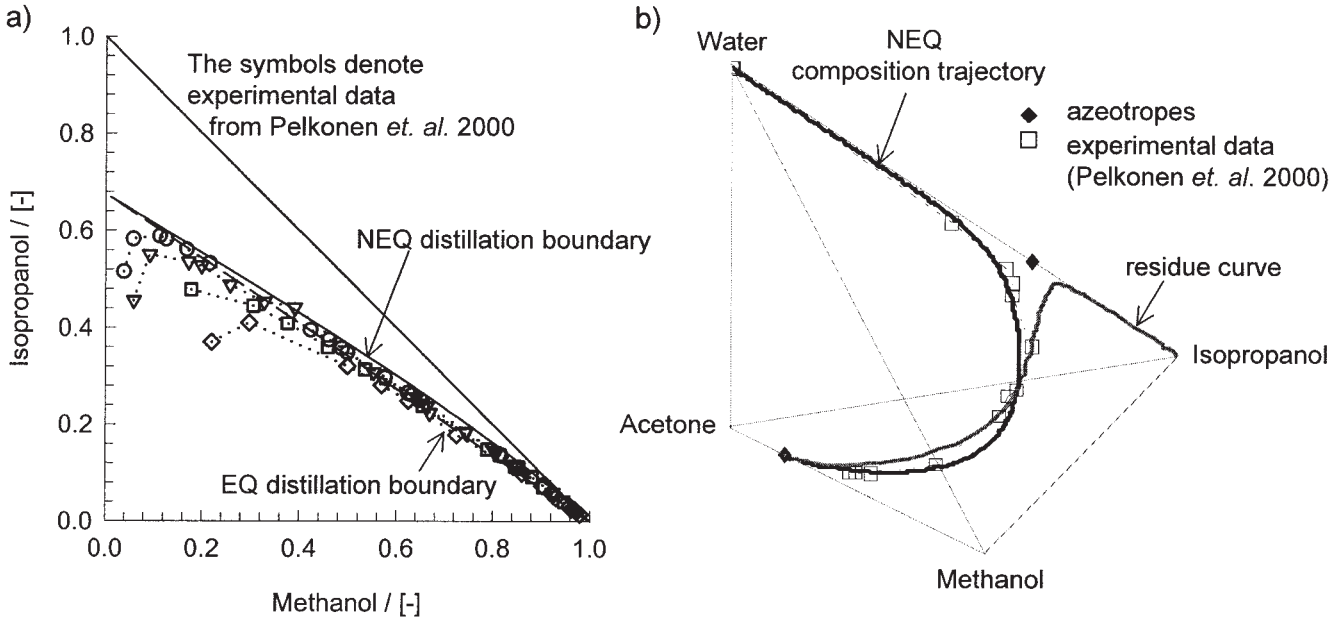

Figure 11. Composition profiles for ternary and quaternary systems in a packed column.

(a) Methanol–water–isopropanol system. (b) Methanol–water–isopropanol–acetone system. Experimental data from Pelkonen et al.[7]

Residue curves and composition curves in tray and packed columns at total reflux may be represented by the following expression (in $c - 1$ dimensional matrix form):

$$\frac{d(x)}{d\eta} = [\Omega](x - y^*) \tag{51}$$

where (y^*) is the matrix of mole fractions of a vapor in equilibrium with the liquid of composition (x) and where

For Residue Curves

$$[\Omega] = [I] \tag{52}$$

For Tray Columns

$$[\Omega] = [I] - [Q] \qquad [Q] = \exp(-[\mathbb{N}_{OV}]) \tag{53}$$

For Packed Columns

$$[\Omega] = [\mathbb{N}_{OV}] \tag{54}$$

These formulas for tray and packed distillation columns rest on the following assumptions:

(1) The resistance to mass transfer in the liquid phase is totally negligible.

(2) The molar flows in the column are constant (this requires the latent heats to be equal and the sensible heat fluxes to be negligible in comparison to the enthalpy fluxes; the latter is very likely in practice).

(3) The temperature of the system is the bubble point temperature of the liquid phase.

The relaxation of the assumptions listed above requires only a moderately more complicated numerical solution to the model equations but would not be expected to lead to significant differences in the results.

The stationary points of these equations are the same (pure components and azeotropes). Thus, mass transfer effects do not change the basic structure of the RCM. However, the boundaries computed from a mass transfer model might not be identical to those computed from the RCM.

The packed and tray column composition trajectories collapse to the residue curves when each species in the vapor phase has an identical facility for mass transfer. That is, all binary numbers of transfer units (mass transfer coefficients) are equal.

$$\mathcal{N}^V_{i,k} = \mathcal{N}^V \qquad i, k = 1, 2, \ldots, c \tag{55}$$

The tray column composition trajectory also collapses to the residue curve when the binary pair vapor phase mass transfer coefficients (or numbers of binary transfer units) approach infinity. Differences between binary pair (M-S) mass transfer coefficients can lead to the composition trajectory taking a direction different from that of the residue curve at the same point in composition space. Differences between residue curves and composition trajectories are characterized by the relative length of and angle between the two composition vectors. The relative length of the composition vectors can be thought of as an average efficiency for a mixture of more than two components. For both types of column this new definition of efficiency has a simple and appealing physical significance: it is the ratio of the arc lengths of the composition trajectory to the arc length of the corresponding residue curve. For a binary system in a tray column this geometric efficiency is equal to the component Murphree efficiencies. For a binary system in a packed column the geometric average efficiency is the overall number of transfer units.

Acknowledgments

The authors thank Harry Kooijman for critical comments and for not insisting that ε be named the multicomponent efficiency.

Notation

a' = interfacial area per unit volume, $m^2\ m^{-3}$
A_c = cross-sectional area of the column, m^2
A_b = bubbling area of tray column, m^2
c_t = total concentration, mol m^{-3}
C = numerical constants
D = Maxwell–Stefan diffusion coefficient, $m^2\ s^{-1}$
E^{MV} = Murphree efficiency
$\Delta H_{i,vap}$ = heat of vaporization of component i, J mol^{-1}
H = height of packing, m
h_f = froth height, m
h = heat transfer coefficient, J $m^{-2}\ K^{-1}\ s^{-1}$
J_i = molar diffusive flux of component i, mol $s^{-1}\ m^{-2}$
K = equilibrium ratio
$[k]$ = matrix of multicomponent mass transfer coefficients, m s^{-1}
$[K_{OV}]$ = matrix of overall multicomponent mass transfer coefficients, m s^{-1}
M = molar hold up, mol
n = number of components
N_i = molar flux transfer rate of component i, mol $s^{-1}\ m^{-2}$
$[\mathbb{N}_{OV}]$ = matrix of overall multicomponent number of transfer units
P = pressure, Pa
$[Q]$ = matrix defined by Eq. 23
q = heat flux, J $m^{-2}\ s^{-1}$
R = gas constant, J $mol^{-1}\ K^{-1}$
$[R]$ = inverse matrix of multicomponent mass transfer coefficients, m^{-1} s
s = arc length of composition curve
T = temperature, K
t = time, s
V = molar vapor flow rate, mol s^{-1}
x_i = mole fraction of component i in liquid phase
y_i = mole fraction of component i in vapor phase
y_i^* = vapor mole fraction of component i in equilibrium with liquid
z_i^α = mole fraction i in phase α

Greek letters

Δ = difference operator
ε = relative length of composition vectors defined by Eq. 42
η = dimensionless length coordinate
$\kappa_{i,k}$ = binary pair mass transfer coefficient components i and k, m s^{-1}
$[\Omega]$ = matrix defined by Eqs. 30–32
τ = dimensionless time

Superscripts

α = denotes phase (V or L)
L = liquid-phase quantity or property
V = vapor-phase quantity or property
$+$ = property of virtual (reference) column in which all species have an equal facility for mass transfer

Subscripts

E = entering
i, j, k = component number
L = leaving
OV = overall (pertaining to both phases)
t = total, summation over all components

Matrix notation

$[\ ]$ = square matrix of order $n - 1$
$[\ ]^{-1}$ = inverse of a square matrix
$(\ )$ = column matrix of dimension $n - 1$

Literature Cited

1. Doherty MF, Malone MF. *Conceptual Design of Distillation Systems*. New York, NY: McGraw-Hill; 2001.
2. Taylor R, Krishna R, Kooijman H. Real-world modeling of distillation. *Chemical Engineering Progress*. 2003;**99**(7):28-39.
3. Taylor R, Krishna R. *Multicomponent Mass Transfer*. New York, NY: Wiley; 1993.
4. Castillo FJL, Towler GP. Influence of multicomponent mass transfer on homogeneous azeotropic distillation. *Chemical Engineering Science*. 1998;53:963-976.
5. Sridhar LN, Maldonado C, Garcia AM. Design and analysis of non-equilibrium separation processes. *AIChE Journal*. 2002;48:1179-1191.
6. Silva JMF, Knoechelmann A, Meirelles AJA, Wolf-Maciel MR, Lopes CE. On the dynamics of nonequilibrium simple batch distillation processes. *Chemical Engineering Processes*. 2003;42:475-485.
7. Pelkonen S, Kaesemann R, Gorak A. Distillation lines for multicomponent separation in packed columns: Theory and comparison with experiment. *Industrial and Engineering Chemistry Research*. 1997;36:5392-5398.
8. Seader JD, Henley EJ. *Separation Process Principles*. New York, NY: Wiley; 1998.
9. Kooijman HA, Taylor R. A Nonequilibrium model for dynamic simulation of tray distillation-columns. *AIChE Journal*. 1995;41:1852-1863.
10. Michelsen M. An efficient general purpose method of integration of stiff ordinary differential equations. *AIChE Journal*. 1976;22:594-597.
11. Bulirsch R, Stoer J. Numerical treatment of ordinary differential equations by extrapolation methods. *Numbers and Mathematics*. 1966;8:1-13.
12. Springer PAM, Buttinger B, Baur R, Krishna R. Crossing of the distillation boundary in homogeneous azeotropic distillation: Influence of interphase mass transfer. *Industrial and Engineering Chemistry Research*. 2002;41:1621-1631.
13. Springer PAM, van der Molen S, Krishna R. The need for using rigorous rate-based models for simulations of ternary azeotropic distillation. *Computers and Chemical Engineering*. 2002;26:1265-1279.
14. Mills AF. *Mass Transfer*. Upper Saddle River, NJ: Prentice Hall; 2001.

Appendix: More on Residue Curves

In this appendix we review three attempts to incorporate mass transfer rate equations in the calculation of residue curves.

Sridhar et al.[5] model

Sridhar et al.[5] begin their analysis of simple batch evaporation in much the same way, as do all others, with the differential material balance for the liquid phase (expressed here in a form slightly different from, but formally equivalent to, that in Sridhar et al.[5])

$$\frac{d(Mx_i^L)}{dt} = -N_i^L a \tag{A1}$$

where M is the liquid holdup, x_i^L is the bulk liquid composition, N_i^L is the molar flux of species i leaving the liquid phase, and a is the area of the vapor liquid interface.

The component material balance for the vapor phase is[5]

$$Vy_i^V = N_i^V a \tag{A2}$$

It follows from Eq. A2 that the bulk vapor composition is given by the ratio of fluxes

$$y_i^V = N_i^V / N_t^V \tag{A3}$$

where N_t^V is the total molar flux. Equation A3, analogous to the conditions at the top of a vertical tube condenser where there is not yet any liquid condensate and the composition of the first droplet, is given by the ratio of molar fluxes (see Chapter 15 of Taylor and Krishna[3]). However, there are some more interesting consequences. If we combine Eq. A3 with the Maxwell–Stefan Eq. 8, assuming that the binary mass transfer coefficients are the same for all pairs of species, we will find that $\Delta y_i = 0$. Further, if the latent heats are equal (often assumed to be true in distillation) then, as discussed in the body of the paper, the total molar flux will be zero and the individual species fluxes will be zero! This implies (see Eq. A1) that the composition of the liquid phase does not change at all!

Clearly these results are at odds with our intuitive understanding of what happens as we heat a flask containing our liquid mixture. We are still in a predicament, even if do not assume the partial molar enthalpies are equal, but neglect the sensible heat terms (a simplification often made)

$$\sum_{i=1}^{n} N_i \Delta H_{i,vap} = 0 \tag{A4}$$

This is the relationship used by Sridhar et al.[5] and implies that the molar fluxes have mixed signs (given that the heats of vaporization have the same sign). That is, some components would evaporate, whereas others would be condensing. But from where do they condense? A possible conclusion is that the sensible heat transfer terms must not be ignored and evaporation cannot be an isothermal process. In fact, evaporation often is modeled as a nonisothermal process (see, for example, Mills[14]). In such models it is often assumed that a liquid evaporates into a gas (such as a pool of water into air or a liquid droplet into a gas stream). The solubility in the liquid phase of the gaseous components is so low that these latter components are assumed to exist only in the gas phase. However, it is important to note that the liquid phase does not evaporate into nothing. Again, this is analogous to the situation in condensation where the sensible heat transfer terms must have a magnitude sufficient to cause the nonzero molar fluxes to have the same sign (direction) (Chapter 15 of Taylor and Krishna[3]).

Let us consider, once again, the actual situation at hand. The temperature of the liquid in the heated flask continues to increase until the mixture reaches its boiling point, at which the first infinitesimally small bubbles of vapor are created. The composition of the vapor in these tiny bubbles is indeed that of a vapor in equilibrium with the liquid. If, as is *assumed* by the standard model of an RCM given by Doherty and Malone,[1] the vapor is removed immediately from any further contact with the liquid, then no further mass transfer can take place. The fact that the rate equations are not needed thus should not come as a complete surprise, and the model as posed by Doherty and Malone[1] is completely consistent.

The above demonstration of the inconsistency in a published nonequilibrium model for an open evaporation rests on an assumption that all species have the same facility for mass transfer. This is unlikely in practice. However, any consistent mass transfer model must allow for that possibility, no matter how unlikely that actual occurrence may be in practice. In any event, we would reach the same conclusion ($\Delta y_i = 0$) even if we use the complete set of M-S equations.

One way out of the difficulties elucidated here is to not require the continuity of fluxes across the vapor–liquid phase boundary. In that event, we would have to consider accumulation of material in the interface itself. Most chemical engineers shy away from attempting to deal with that eventuality in an engineering model!

The Silva et al.[6] model

The analysis developed above strongly suggests that a recent paper by Silva et al.[6] would also appear to be incorrect. Silva et al.[6] begin from the material balance Eqs. 1 and A2, and the following expression for the molar flux in the vapor film

$$N_i^V = \frac{1}{RT} k_i^V (P^I y_i^I - P y_i^V) \tag{A5}$$

where P^I is the pressure at the vapor–liquid interface and P is the pressure in the bulk vapor. Equation A5 is a somewhat unconventional form for the vapor-phase rate equation but it can be written in the following equivalent, and more recognizable, form

$$N_i^V = \frac{1}{RT} k_i^V (p_i^I - p_i^V) \tag{A6}$$

There is nothing particularly unusual about the choice of partial pressure driving forces for gas-phase mass transfer. It should also be noted that Silva et al.[6] neglect the liquid-phase resistance to mass transfer in their model (there is nothing unusual in that assumption either).

Silva et al.[6] state that because they do not consider the energy equation, their development applies to isothermal processes. This is misleading; the interfacial energy balance applies to isothermal processes just as much as it applies to nonisothermal processes. Their calculations are carried out at constant (specified) temperature. The consequence is that the pressure (rather than the temperature) must be determined during the calculations. There is nothing fundamentally wrong with this procedure, although residue curve calculations normally are carried out at constant (specified) pressure (if for no other reason than that it is rather more useful to process design than is an isothermal RCM). What is very unusual is the assumption by Silva et al.[6] that the total pressure at the interface differs from that in the bulk vapor phase. In their procedure Silva et al.[6] calculate the interface pressure from a standard bubble point calculation. Because their illustrative calculations are for ideal systems only, the interface pressure is calculated directly using an expression that can be derived using Raoult's law

$$P^I = \sum_{i=1}^{n} x_i^L P_i^* \tag{A7}$$

where P_i^* is the (known or easily estimated) vapor pressure of species i at the specified system temperature. The pressure in the bulk vapor phase is calculated from

$$\sum_{i=1}^{n} \frac{k_i^V P^I y_i^I a}{RTV + k_i^V P^V a} = 1 \tag{A8}$$

This relation, derived from the fact that the mole fractions in the bulk vapor phase must sum to unity, normally will lead to a bulk vapor-phase pressure that differs from that at the surface. Although it is entirely to be expected that there will be *partial* pressure differences over the film, *total* pressure changes normally lead to bulk fluid flow, not to mass transfer by molecular diffusion. In fact, it is far more likely for the process to be isobaric, than for it to be isothermal; pressure equilibrium normally is established fairly rapidly in any real process. It is standard practice in mass transfer models to assume that the pressure is constant, at least over any thin film adjacent to a phase boundary. Thus, their model is highly unusual to say the least.

Silva et al.[6] state that their model is equivalent to that of Doherty and coworkers if the process is isobaric (rather than isothermal) *and* the vapor flow is zero. This is incorrect. It may be true that Doherty and many others compute RCMs at constant pressure (for the reasons given above), but that does not mean that the vapor flow rate is zero because that requires the liquid composition to remain constant so as not to violate the bulk liquid material balance Eq. 1.

We could (and should) assume constant pressure over the film, in which case the rate Eq. A6 simplifies to

$$N_i^V = c_t^V k_i^V (y_i^I - y_i^V) \tag{A9}$$

where $c_t^V = P/RT$ is the molar density of the vapor phase as given by the ideal gas equation of state. This is the dilute solution approximation of the M-S equations, valid when all species but one are present in very low relative amounts (see Chapters 6 and 8 of Taylor and Krishna[3]). Equation A9 is very widely used in mass transfer modeling (even in conditions for which it does not apply). Let us further assume that the heats of vaporization are the same for all species (we admit that this might be unlikely, but it is a possibility that we must be able to accommodate); then the simplified energy balance becomes

$$\sum_{i=1}^{n} k_i^V \Delta y_i = 0 \tag{A10}$$

However, because the mole fraction driving forces sum to zero, this relationship cannot always be satisfied unless all of the mass transfer coefficients have the same value. The real problem is the use of Eq. A9 for each species in the mixture. In fact, only $n - 1$ mass transfer rate equations can be used in a mass transfer model. Although it appears as though Silva et al.[6] integrate the requisite number of $n - 1$ combined material balance/rate equations, their entire procedure requires values for n mass transfer coefficients (see Eq. A8). In their illustrative calculations for three component mixtures, Silva et al.[6] assign numerical values to three vapor-phase mass transfer coefficients (they are provided in the figure captions). In all but one case, the numerical values differ from each other, although in no case do they satisfy Eq. A10. In one of their examples, the ratio of largest to smallest mass transfer coefficient is no less than 4 orders of magnitude. This ratio is at least 2.5 orders of magnitude larger than anything that could be encountered in any real mixture! It is worth noting that the M-S equations correctly sum over all species to zero, provided only that the values of the binary M-S mass transfer coefficients satisfy the symmetry requirement $\kappa_{i,k}^{\alpha} = \kappa_{k,i}^{\alpha}$.

In view of the foregoing inconsistencies in their model and calculation procedure, we believe that the computational results and conclusions of Silva et al.[6] should be regarded as incorrect.

Castillo and Towler[4] model

The compositions of the vapor and liquid phases leaving a tray in a real distillation column are not in equilibrium with each other. One way to account for departures from equilibrium in tray distillation columns is through the use of an efficiency factor. Castillo and Towler[4] use a Murphree-type efficiency and write (for total reflux conditions)

$$y_i = (1 + E_i^{MV} K_i - E_i^{MV}) x_i \tag{A11}$$

This is the relationship used by Castillo and Towler[4] in conjunction with the material balance (Eq. 2) to relate the composition of the vapor and liquid phases. Assuming (or computing) values for the component efficiencies allows us to integrate the differential material balance relations.

The problem with this approach is that the above expression applies to a steady-state countercurrent flow process in which vapor and liquid phases are deliberately brought into contact with one another. This is very different from the model of simple distillation described by Doherty and Malone.[1] However, there is no similar inconsistency in the use of an efficiency model in their calculation of distillation lines. Their method then bears a relationship to that described in this paper, except that the method described here does not have to deal with unbounded efficiencies.

Manuscript received Dec. 12, 2003, and revision received Apr. 15, 2004.